Field Crops Research 289 (2022) 108710

Contents lists available at ScienceDirect

Field Crops Research

journal homepage: www.elsevier.com/locate/fcr

Spectral assessments of N-related maize traits: Evaluating and defining agronomic relevant detection limits

Paul Heinemann *, Urs Schmidhalter

Technical University of Munich, Chair of Plant Nutrition, Emil-Ramann-Str. 2, Freising, Weihenstephan 85354, Germany

ARTICLE INFO

Keywords:
Agronomical error limits
Drone
Nitrogen fertilization
Precision agriculture
Remote sensing

ABSTRACT

Summary: The spectral sensing of nitrogen (N)-related traits and the grain yield of maize (*Zea mays* L.) is widely used in agricultural practice because it is rapid, non-destructive, and cost-efficient. However, there exists a lack of agronomically supported spectral detection limits. The agronomic aspects have not yet been fully considered based on commonly used statistical measures such as the coefficient of determination (R^2), the root-mean-square error (RMSE), and the mean absolute error (MAE) and should therefore be extended. In the present study, we evaluated regression models of spectral indices derived from an unmanned aerial vehicle (UAV) by capturing N-related traits such as above-ground and grain N uptake, the nitrogen nutrition index (NNI), and grain yield covering data sets of two years, sites, and four developmental stages of maize. The results suggest that an agronomic evaluation exclusively adopting widely used statistical measures is not fully adequate. The R^2 is essentially influenced by differentiation of the trait, which in turn depends on year effects and growth stages. Further statistics such as RMSE and MAE average the error and lead to an under- and overestimation for most observations. In this investigation, we defined an appropriate agronomical error interval for above-ground and grain N uptake, NNI, and grain yield of $\pm$ 40 and $\pm$ 25 kg N ha^{-1}, $\pm$ 0.2, and $\pm$ 1.4 t ha^{-1}, with a probability of at least 80%. These interval limits are consistent across years and growth stages. The consistency occurs because most spectral indices are dominated by biomass. Across all of them, the best-performing spectral indices combine GREEN, REDEDGE, and NIR bands. For spectral indices using the RED band, the range of the agronomic error interval performed equally with a slightly worse probability of data points inside the error limits. Agronomically based error limits should be included in addition to common statistical measures in the spectral assessment of N-related traits of maize and grain yield to optimize the ex-ante and/or ex-post analysis of N-fertilization.

1. Introduction

Maize (*Zea mays* L.) is one of the world's key cereal crops, along with rice and wheat. Maize is used in various food, feed, and industrial products (Awika, 2011; Ranum et al., 2014). In 2020, one-third of farms worldwide cultivated maize, and it is estimated that the number of maize-growing farms will increase by 5% in 2030, by which time maize will have overtaken wheat in terms of growing area (Erenstein et al., 2021).

Since maize production is often limited by N, additional N-fertilization will have to be applied in most cases (Ladha et al., 2005). N has a major role in influencing the yield and quality of crops (Mason and D`Croz-Mason, 2002; Robertson and Vitousek, 2009; Chen et al., 2015), but maize is able to use only a small amount of the applied N (Raun and Johnson, 1999; Ladha et al., 2005; Barbieri et al., 2008). Some of the N applied is released into the air, water, and land, causing environmental and human health problems (Galloway et al., 2008). Minimizing N losses by optimizing N-fertilization is, therefore, necessary.

Especially in arable maize cropping systems, many tools are available for improving nitrogen use efficiency (NUE) and avoiding N losses, e.g., the adaption of source, method, rate, and timing of N-application, remediation of soil acidity, controlled release of N through urease- and nitrification inhibitors, tillage system, use of animal and green manure, water management, crop rotation, crop residue management, cover crops, and the use of N efficient species and genotypes, as well as the control of biotic pests (Fageria and Baligar, 2005).

N-fertilizer requirement determinations are based on expected grain yields, which can vary widely between years (Berenguer et al., 2009). In Europe, the mineral N-fertilization is often carried out through band application at the planting time. An additional broadcast application is

* Corresponding author.
E-mail address: schmidhalter@wzw.tum.de (U. Schmidhalter).

https://doi.org/10.1016/j.fcr.2022.108710
Received 1 April 2022; Received in revised form 2 October 2022; Accepted 4 October 2022
Available online 14 October 2022

frequently made during the early leaf development (up to the seven-leave stage) due to the low clearance of tractors and possible etching damage to maize plants. Organic N-fertilizers are also applied either before sowing or early in the maize growing season. However, at these developmental stages, the total N requirement of maize cannot yet be estimated. One commonly used method of better estimating the N needs early in the season is the determination of the soil residual nitrogen (nitrate-N + ammonium-N, "Nmin") already present in the soil (Heinemann and Schmidhalter, 2021). However, maize exhibits a considerable N uptake only in the later stages of development, and differentiation of the N uptake due to treatment effects (e.g., different N-fertilization) often occurs only later in the growing season (Ciampitti and Vyn, 2011). Additionally, using organic fertilizers is very effective in maize (Dordas et al., 2008). In this context, interest also exists in mapping the availability of N in long-term organically fertilized fields. Therefore, recording the above-ground N uptake, grain N uptake, the nitrogen nutrition index (NNI), and maize grain yield during vegetation is also important when evaluating the preceding N-fertilizer actions. The NNI expresses the relationship between the N content and the above-ground dry matter. NNI values ≥ 1 indicate a current N content that does not impede biomass growth, whereas values < 1 indicate a limitation of biomass production due to a currently insufficient N content (Plénet and Lemaire, 1999).

One common major method used to detect the N-status is the optical, non-destructive measurement of the plant canopy reflectance signature (Schmidhalter et al., 2001; Mistele and Schmidhalter, 2008; Winterhalter et al., 2011; Ali et al., 2017). The main measurement range of the sensors is between the wavelengths of 400 and 1000 nm. In this spectral range, the vegetation shows a typical reflection signature which is controlled in the visible wavelength range (400–700 nm) by the absorption of pigments (mainly chlorophyll *a* at 430/660 nm and chlorophyll *b* at 450/640 nm, as well as other pigments such as carotenoids and xanthophylls at 450 nm) and in the near-infrared (700–1100 nm) by reflection processes in the foliar layers (Lilienthal, 2014). Since N-fertilization affects the plant's aforementioned physiological parameters, N-related traits such as the above-ground and grain N uptake, grain yield, and NNI of maize lend themselves well to spectral recording (Walburg et al., 1982; Mistele and Schmidhalter, 2008; Xia et al., 2016).

Many spectral indices are available for detecting N-related traits in maize, with each differing in both the spectral range (visible, red edge, near-infrared) and wavelengths used (normalized difference, simple ratio). Many studies have observed good maize performance in the spectral detection of N uptake (Mistele and Schmidhalter, 2008; Li et al., 2014; Li et al., 2020), grain N uptake (Becker et al., 2020), NNI (Zhao et al., 2018), and grain yield (Osborne et al., 2002; Maresma et al., 2016; García-Martínez et al., 2020).

Ground-based systems such as handheld sensors (Teal et al., 2006; Thompson et al., 2015), sensors mounted on carrier vehicles (Mistele and Schmidhalter, 2008; Winterhalter et al., 2013), and, more recently, airborne systems such as unmanned aerial vehicles (UAV) (Zaman-Allah et al., 2015, Gnädinger and Schmidhalter, 2017; de Souza et al., 2021) or satellites (Kayad et al., 2019; Skakun et al., 2021) have been able to be used for spectral measurements. The advantages of UAVs over ground-based systems include the ability to measure without disrupting the surface, capturing spatial information simultaneously, and generating high-resolution images (Aasen and Bolten, 2018). Compared to satellite imagery, the UAV has the advantage of smaller ground sample distances (Hunt and Daughtry, 2018).

Regression models are frequently calculated between spectral indices (independent variables) and agronomic traits (dependent variables). In a further step, the regression function will be used to estimate the dependent variable. The quality of the estimation is often assessed by statistics such as the coefficient of determination (R^2), the root-mean-square error (RMSE), and the mean absolute error (MAE). The regression model is assumed to estimate the dependent parameters well when high R^2 and low RMSE and MAE values occur (Lee et al., 2020; Zhang et al., 2020). However, especially in agronomic applications such as in-season management decisions (ex-ante analysis, e.g., N-fertilization) as well as the ex-post analysis of actions already implemented (which also provide useful information), the error limits of the model should be taken into account from an agronomical point of view. For example, agronomic aspects may include the site-specific N-fertilization level and the acceptable error of the actual maize trait analyzed. The user-defined error limits can then be evaluated based on the proportion of data points inside or outside the interval, thus providing information on the model's applicability to agricultural applications.

Therefore, this study (i) spectrally assesses N-related traits (above-ground and grain N uptake, NNI), as well as the grain yield of maize at the canopy level, (ii) determines the sensitivity of spectral indices in detecting N-related traits of maize while taking into account the developmental stage, (iii) compares different statistical measures of goodness indicating the performance of regression models assessing the spectral detection of N-related traits, (iv) and evaluates and expands the statistical measures from an agronomical point of view to match agricultural needs.

2. Materials and methods

2.1. Field trials

In 2018 and 2019, field experiments were conducted at the Dürnast research station of the Technical University of Munich in Germany (48°23′60″ N, 11°41′60″ E). The soil of the directly adjacent experimental fields consists of a mostly homogeneous Cambisol with a silty-clay loam texture. The average annual temperature is 8 °C, and the average precipitation is approximately 800 mm.

Maize (*Zea mays* L., variety Amagrano) was sown on 25.04.2018 with 11 and 17.04.2019 with nine kernels per square meter. In both years, the preceding crops had been winter wheat. The fields were managed conventionally, and plant protection activities were in line with local standards. Potassium and phosphorus were supplied through fertilization as part of the crop rotation. The nitrate-N content of the 0 −60 cm soil layer was measured at the vegetation beginning and amounted to 43 and 49 kg ha^{-1} in 2018 and 2019, respectively. The experimental fields did not receive organic fertilization in the experimental year or in previous years.

The experiments were set up in 2018 as a completely randomized design with six repetitions and in 2019 as a double-created Latin square design with each of four repetitions. The experimental designs were chosen in 2018 due to the region-specific rather small field size and in 2019 due to possible topographical influence and the prevention of effects through previous experiments. The plot length was 20 m and 15 m in 2018 and 2019, respectively, and the width was 12 m. These large plot sizes avoid edge effects and can be managed with conventional agricultural technics. Both test designs met the requirements for the subsequent data analysis.

In both years, N-fertilizer was applied once at the rates of 0, 80, 120, and 160 kg N ha^{-1} during the leaf development stage (BBCH 13–19; the BBCH score indicates the developmental stage and is the abbreviation for ***B**iologische **B**undesanstalt für Land- und Forstwirtschaft, Bundessortenamt und **CH**emische Industrie*, Meier, 2018). The N-fertilizer forms were ammonium sulfate urea (39% N) and ammonium sulfate nitrate (26% N) in 2018 and 2019, respectively. They were applied using a pneumatic spreader (Rauch® AERO, Germany) in 2018 and, in 2019, precisely dosed and distributed with a box spreader (Fiona® G-85, Denmark). The range of the fertilized N levels, 80−160 kg N ha^{-1}, reflects the relevant range of N-fertilization in agricultural practice for the yield expectations typical of this site (Lfl, 2018). A further treatment without N-fertilization (0 kg N ha^{-1}) was used to obtain additional information on the site and the year-specific N supply due to soil N mineralization.

2.2. Spectral measurements

Spectral aerial-based measurements (UAV) were conducted under cloud-free conditions and directly after destructive data collection, except for the measurement date at BBCH 86 in 2019, when spectral sensing was made seven days before the destructive sampling. Aerial-based multispectral sensing was performed using an eBee and eBee RTK fixed-wing aircraft (SenseFly®, Lausanne, Switzerland). These UAVs were equipped with the same multispectral camera (Sequoia$^+$ camera, Parrot, Paris, France), which recorded four spectral bands of the electromagnetic spectrum: GREEN (550 nm, ~40 nm bandwidth), RED (660 nm, ~40 nm bandwidth), REDEDGE (735 nm, ~10 nm bandwidth), and NIR (790 nm, ~40 nm bandwidth). A white balance card was used to calibrate the reflectance. The flights were carried out in 2018 at an altitude of 80 m, resulting in ground resolutions of about 8 cm/pixel. Due to the presence of adjacent trees, this was the minimum possible flight altitude. In 2019, aerial surveys could be conducted at 55–60 m above the ground surface, resulting in a 5 cm/pixel ground resolution. The individual images were merged using Pix4D software (Pix4D S.A., Prilly, Switzerland). Further details on the UAV equipment can be found in Hu et al. (2020). A polygon for each plot was subsequently created for the complete image of each band using ArcGIS (ESRI®, Germany, Version 10.5.0.6491). Peripheral areas and biomass harvesting areas of each plot were excluded. The mean value per polygon was then calculated for each band. At the first sampling date in 2019 (BBCH 36), three plots from the complete spectral image were removed from further analysis due to artifacts.

From the reflectance data, commonly used indices were calculated (Table 1), including wavelengths related to maize traits (Mistele and Schmidhalter, 2008; Zhao et al., 2018; García-Martínez et al., 2020; Ramos et al., 2020).

2.3. Destructive data collection, laboratory analyses, soil sampling, and further calculations

For the determination of the above-ground N uptake of maize, plant samples were taken in the core of each plot at indicative developmental stages at BBCH 51 and 61 in 2018 and BBCH 36 and 86 in 2019. Totally 16 plants were manually harvested from two adjacent rows. Subsequently, the fresh plant samples were separated into leaves, stems, and – in 2019 at BBCH 86 – additionally into cobs and then chopped. For grain yield determination, two interior rows 20 and 15 m in length of each plot were threshed in 2018 and 2019, respectively (Deutz-Fahr®, Germany). A subsample of each sample was oven-dried at 60 °C until no further water loss occurred, then weighed to determine the above-ground dry weight (DW). The dried plant samples were then milled and sieved to 0.5 mm (Brabender®, Duisburg, Germany) for subsequent analysis in the laboratory to determine the N content (%). This was done by mass spectrometry using an isotope radio mass spectrometer with an ANCA SL 20–20 preparation unit (Europe Scientific, Crewe, UK).

The above-ground total plant N uptake (kg N ha^{-1}) was calculated as DW x N content for stems, leaves, and, if available, cobs, then summed up and expressed per hectare. For grain yield calculation, the harvested area was determined, and the sample weight was converted to yield per hectare with 14% moisture. To characterize the N supply of maize at each measurement date, the NNI was calculated according to Lemaire and Gastal (1997) and is expressed as:

$$\mathrm{NNI} = \frac{\mathrm{Nact}}{\mathrm{Nc}} \quad (1)$$

where N_{act} (%) is the actual measured N content, and N_c (%) is the critical N content of the shoot dry matter. For N_c, Plénet and Lemaire (1999) developed the following estimation equation:

$N_c = 3.40$ (shoot dry weight [t ha^{-1}]$^{-0.37}$),

which was based on investigations of maize when the shoot dry weight was in the range of 1.0–22.0 t ha^{-1}, and growth stages ranged from emergence till silking + 25 days. NNI values ≥ 1 indicate no limitation of biomass production since there was sufficient N content, whereas NNI values < 1 indicate a limitation of biomass limitation due to insufficient N content. The NNI was not calculated for BBCH 86 in 2019 due to the function restriction at this growth stage.

In each plot, soil samples for nitrate-N analysis were taken at the beginning of vegetation (VB) before N-fertilization and after the harvest using a tractor-mounted soil sampling device down to a 60 cm soil depth in 30 cm increments. Chemical analysis was performed using high-performance liquid chromatography (HPLC). A dry bulk density of 1.5 g cm^3 was assumed for the calculation of the soil nitrate-N content (Heinemann and Schmidhalter, 2021).

2.4. Statistical analysis

The data were analyzed using Microsoft® Excel® 2019 MSO (16.0.14701.20240) and R (2021).

Based on the Akaike Information Criterion (AIC) (Webster and McBratney, 1989), either linear or polynomial (second-order) regressions were calculated between each of the dependent variables (above-ground N uptake, grain N uptake, NNI, and grain yield) and the indices, respectively. The coefficient of determination (R^2) was calculated as a measure of goodness of fit. R^2 shows the portion of the explained variance in the model concerning the total variance (Eq. 2):

$$R^2 = \frac{explained \quad deviation \quad sum \quad of \quad squares}{total \quad deviation \quad sum \quad of \quad squares \quad to \quad be \quad explained} = \frac{\sum_{i=1}^{n} (\hat{y}i - \bar{y})^2}{\sum_{i=1}^{n} (yi - \bar{y})^2} \quad (2)$$

where $\bar{y}$ is the arithmetic mean of all observed y_i and $\hat{y}_i$ is the estimator

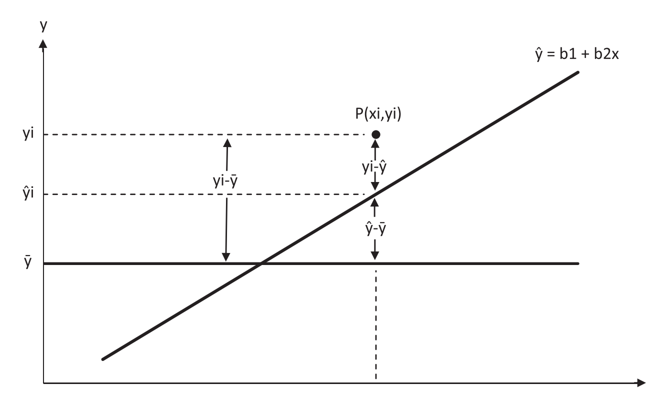

Fig. 1. Diagram showing the decomposition of the deviation sum of squares: x and y represent the independent and dependent variables with P as an example of one single measured value; $\bar{y}$ is the arithmetic mean of all observed y_i, and $\hat{y}_i$ is the estimator (regression function) of each observed y_i (according to Bleymüller et al., 2008).

Table 1
List of indices recorded with a UAV. The original bands were approximated depending on the technique used.

Index	Equation	Reference
NDVI	$\frac{R790 - R660}{R790 + R660}$	Rouse et al. (1974)
NIR/GREEN	R780/R550	Mistele and Schmidhalter (2008)
NIR/RED	R780/R670	Gitelson et al. (2003)
NIR/REDEDGE	R780/R735	de Souza et al. (2021)
NDRE	$\frac{R790 - R720}{R790 + R720}$	Barnes et al. (2000)

(regression function) of each observed y_i. Fig. 1 illustrates these relationships graphically.

As a further measure of the predictive quality of the regression, the confidence interval (95% level) for the estimated value (regression estimator) and the prediction interval (95% level) for the observed value is commonly used in statistics. A detailed description can be found in Bleymüller et al. (2008) and Köhler et al. (2012).

To obtain a more specific evaluation of the error of the entire model, the root mean square error (RMSE) was calculated as follows:

$$\text{RMSE [kg N } ha^{-1}] = \sqrt{\frac{\sum_{i=1}^{n} (\hat{y}_i - y_i)^2}{n}} \tag{3}$$

where $\hat{y}_i$ are the predicted and y_i the measured values for the N uptake and n the number of samples. The advantage of RMSE is that it uses the same data unit as the variable to be explained. To enable better comparability of RMSE with other data sets, the RMSE values were standardized as a percentage and calculated as follows (modified according to Loague and Green, 1991):

$$\text{RMSE [\%]} = \sqrt{\frac{\sum_{i=1}^{n} (P_i - O_i)^2}{n}} \times \frac{100}{\bar{O}} \tag{4}$$

where P_i and O_i are the predicted and observed values and n the number of samples. $\bar{O}$ represents the mean of the observed data. The RMSE values were then classified and evaluated according to Westermeier and Maidl (2019). RMSE values < 10% were considered excellent, 10–20% good, and > 30% sufficient.

Another generally accepted error in the entire model is the mean absolute error (MAE), which was calculated as follows:

$$\text{MAE [kg N } ha^{-1}] = \frac{\sum_{i=1}^{n} |P_i - O_i|}{n} \tag{5}$$

where P_i and O_i are the predicted and observed values, and n is the number of samples. For a detailed description of RMSE and MAE, the reader is referred to Willmott (1984).

In addition to the commonly accepted statistical error measures for regressions, confidence intervals were calculated that tolerate an acceptable model error from an agronomic point of view. The magnitude of the error depends mainly on the trait of maize and the growth stage. This error is calculated using:

$$\text{agronomic error [unit of the trait of maize]} = \hat{y}_i \pm \text{error of } y_i \tag{6}$$

where $\hat{y}_i$ is the estimator of the regression function and y_i is the agronomic error. To evaluate the size of the error, sensitivity analyses were performed for the best performing index (based on the conventionally used statistics) at each trait*date combination. As a measure of goodness, the proportion of data points that fell outside the interval was chosen, and we imply that a reasonable value is maximally 20%. Based on this, we assumed ± 40 kg ha^{-1} for above-ground N uptake, ± 25 kg ha^{-1} for grain N uptake, ± 0.2 units for NNI, and ± 1.4 t ha^{-1} for grain yield.

3. Results

3.1. Weather conditions, plant development, and treatment effects

The weather in 2018 and 2019, as detected from a weather station located nearby (Climate Data Center (CDC), 2020), showed some significant deviations during some months from the long-term average (mean 1981–2010), which influenced the maize growth (Fig. 2). In both experimental years, the temperature was above the long-term average,

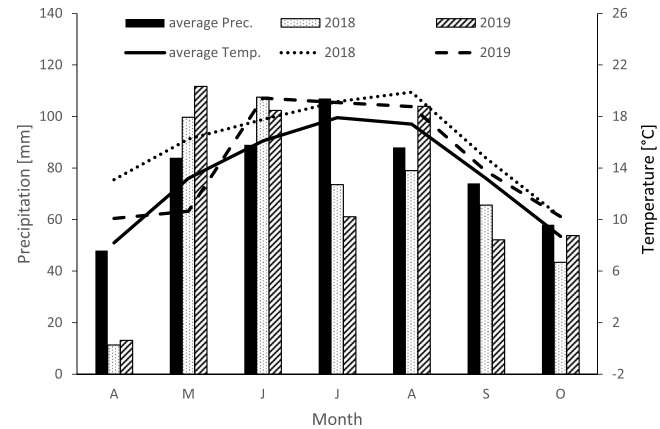

Fig. 2. Monthly weather conditions (April to October) at the experiment site in 2018 and 2019 compared to the long-term average (1981–2010). The temperature (Temp.) is shown as lines and precipitation (Prec.) as bars (CDC, 2020).

except for below-average temperatures during May 2019. Averaged across all months, 2018 deviated further from the long-term average. In 2018, less precipitation was observed during April and July and the entire period from August to October, with more precipitation in May and June. In 2019, much less precipitation was observed in April, July, August, and September and more in May, June, and August compared to the long-term average. Averaged across all months, a precipitation deficit was observed in both years compared to the long-term average (550 mm). In contrast, the total precipitation for 2018 (480 mm) and 2019 (498 mm) hardly differed from the observation period.

The soil nitrate-N contents are presented in Table 2. No significant differences across the N levels were observed at the beginning of vegetation in both years and during 2018 after harvest. In contrast, increasing N-fertilization resulted in significant differences in 2019.

Across all measurement dates, the total above-ground N uptake, grain N uptake, NNI, and grain yield showed ranges of 307 kg N ha^{-1}, 107 kg N ha^{-1}, 0.97, and 7.0 t ha^{-1} with minimum values of 67 kg N ha^{-1}, 90 kg N ha^{-1}, 0.53, and 8.7 t ha^{-1} and maximum values of 375 kg N ha^{-1}, 197 kg N ha^{-1}, 1.50, and 15.7 t ha^{-1}, all respectively (Figs. 3 and 4).

The grain yield differed significantly between the unfertilized and fertilized treatments only in 2019 (Fig. 3a). Significant differences in grain N uptake were observed during both years among the N levels. The increase in grain N uptake decreased with increasing N-fertilization (Fig. 3b).

The above-ground N uptake (Fig. 4a) and NNI (Fig. 4b) differentiated hardly across the N levels in 2018 at BBCH 51. Significant differences between the unfertilized variant and the fertilized variants were only

Table 2
Nitrate-N mean measured in 0–60 cm soil depth at the beginning of vegetation (VB) and after harvest in 2018 and 2019 indicated for the different N-fertilization levels. The standard deviation is shown in brackets. Different letters indicate significant differences between the N levels within each sampling date*year combination (Tukey test, p-value = 0.05).

Date	N-Fertilization [kg N ha^{-1}]	Year	
		2018	2019
VB	0	39.2 (4.83) a	52.6 (6.98) a
	80	41.9 (12.26) a	46.1 (6.95) a
	120	41.2 (14.38) a	48.5 (6.07) a
	160	54.8 (28.47) a	48.1 (5.37) a
Post-harvest	0	15.4 (5.48) b	3.8 (4.64) a
	80	31.7 (13.97) b	4.5 (3.47) a
	120	53.8 (38.51) ab	7.5 (9.08) a
	160	75.9 (26.60) a	3.7 (1.74) a

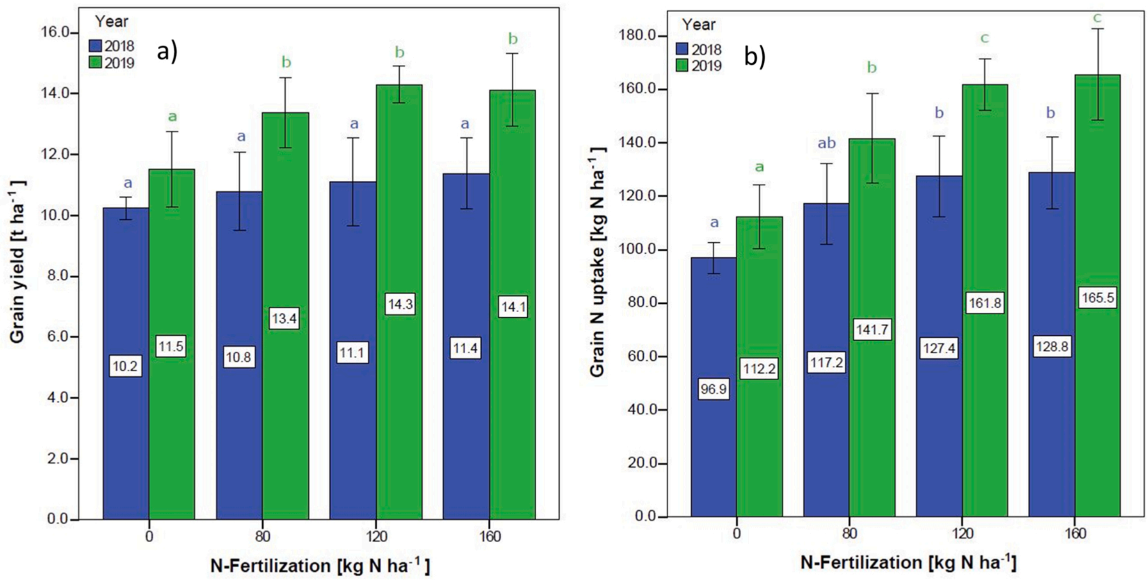

Fig. 3. Comparison of the traits (a) grain yield (t ha^{-1}, 14% water content) and (b) grain N uptake (kg N ha^{-1}) of maize across 2018 and 2019. Different letters indicate significant differences between the N levels within each trait*year combination (Tukey test, p-value = 0.05). The standard deviation is shown as bars.

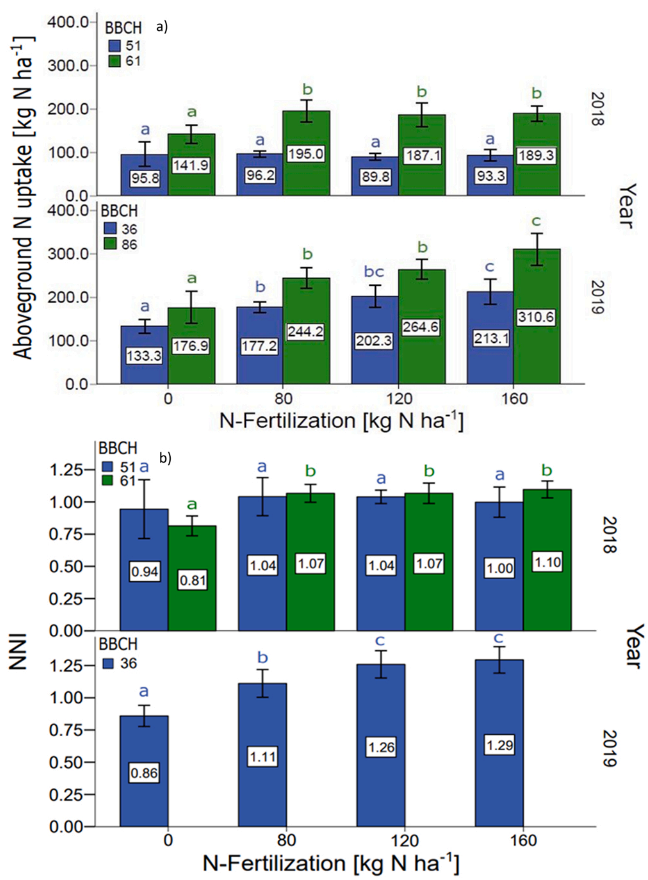

Fig. 4. Differentiation of the traits (a) above-ground N uptake (kg N ha^{-1}) and (b) NNI values of maize on the respective sampling dates (BBCH-codes) indicated separately for the years 2018 and 2019. Different letters indicate significant differences between the N levels within each sampling date*year combination (Tukey test, p-value = 0.05). The standard deviation is shown as bars.

observed at BBCH 61. On both measurement dates, the maximum N uptake and NNI were already achieved with an N-fertilization of 80 kg N ha^{-1}. In 2019, a significant differentiation in N uptake and NNI across the N levels were evident at BBCH 36 and 86. Higher N-fertilization increased both N uptake and NNI.

3.2. Comparison of spectral reflectance and indices

Reflectance signatures at each measurement date*year combination for the corresponding N levels differed hardly in 2018, whereas the GREEN, REDEDGE, and NIR bands deviated most at both measurement dates in 2019. In addition, the strongest deviation was observed for the REDEDGE band at BBCH 86 (data not shown).

Spectral indices were calculated based on the reflectance data and used as independent variables to estimate maize traits using regression models (Tables 3–6). In general, linear regressions were mainly obtained, whereas the indices, including REDEDGE and NIR bands, frequently delivered polynomial regression functions. Across all, the best performing indices were the NDRE, NIR/REDEDGE, and NIR/GREEN, followed by the NDVI and NIR/RED indices. Although some indices differed more in R^2 values on the given measurement dates, other statistical measures showed smaller differences as being rather negligible from an agronomic point of view.

3.3. Defining agronomically relevant error limits

The proportion of data points (%) outside the interval considered agronomically relevant was calculated based on the best performing index using conventional statistics at each date*trait combination (Fig. 5).

Given a reasonable error of 20% of data points outside the agronomically relevant interval, the reasonable limits adopted for the spectral assessment of above-ground and grain N uptake, the NNI, and grain yield were ± 40 kg N ha^{-1}, ± 25 kg N ha^{-1}, ± 0.2, and ± 1.4 t ha^{-1} across all measurement dates.

3.4. Evaluation of the spectral assessment of the above-ground and grain N uptake, NNI, and grain yield through regression analysis

The regression models between the UAV-derived spectral indices and the traits of above-ground N uptake (Table 3), grain N uptake (Table 4),

Table 3
Comparison of statistical measures of goodness depicting the spectral assessment of maize above-ground N uptake [kg N ha^{-1}] in different years and development stages (** ≙ $p < 0.01$, and *** ≙ $p < 0.001$). $\hat{y}_i$ is the estimator of the polynomial (poly) and linear (lin) regression function at the point x_i.

Year	BBCH	Index	Type of Regression	R^2	RMSE [kg N uptake ha^{-1}]	RMSE [%]	MAE [kg N uptake ha^{-1}]	Proportion of data points (%) outside of the agronomically relevant interval [$\hat{y}_i \pm 40$ kg N uptake ha^{-1}]
2018	51	NDVI	lin	0.03 * **	15.0	16.0	10.5	4.2
2018	51	NDRE	lin	0.07 * **	14.7	15.6	10.2	4.2
2018	51	NIR/GREEN	lin	0.07 * **	14.7	15.7	10.0	4.2
2018	51	NIR/RED	lin	0.04 * **	14.9	15.9	10.4	4.2
2018	51	NIR/REDEDGE	lin	0.08 * **	14.7	15.6	10.2	4.2
2018	61	NDVI	lin	0.03 * **	29.7	16.6	23.3	25.0
2018	61	NDRE	poly	0.15 * **	27.8	15.6	23.8	12.5
2018	61	NIR/GREEN	lin	0.01 * **	30.0	16.8	23.7	29.2
2018	61	NIR/RED	lin	0.03 * **	29.7	16.6	23.4	25.0
2018	61	NIR/REDEDGE	poly	0.14 * **	27.8	15.6	23.9	12.5
2019	36	NDVI	lin	0.23 * **	33.1	18.1	26.1	27.6
2019	36	NDRE	lin	0.45 * **	28.1	15.4	22.8	10.3
2019	36	NIR/GREEN	lin	0.50 * **	26.7	14.6	21.4	13.8
2019	36	NIR/RED	lin	0.27 * **	32.3	17.6	25.9	27.6
2019	36	NIR/REDEDGE	lin	0.44 * **	28.2	15.4	22.8	13.8
2019	86	NDVI	lin	0.56 * **	36.9	14.9	28.8	31.3
2019	86	NDRE	lin	0.73 * **	28.9	11.7	22.1	21.9
2019	86	NIR/GREEN	lin	0.65 * **	32.7	13.2	25.6	31.3
2019	86	NIR/RED	lin	0.56 * **	36.9	14.9	29.9	28.1
2019	86	NIR/REDEDGE	lin	0.73 * **	28.8	11.7	22.2	21.9

Table 4
Comparison of statistical measures of goodness depicting the spectral assessment of maize grain N uptake [kg N ha^{-1}] in different years and development stages (* ≙ $p < 0.05$, ** ≙ $p < 0.01$, and *** ≙ $p < 0.001$). $\hat{y}_i$ is the estimator of the polynomial (poly) and linear (lin) regression function at the point x_i.

Year	BBCH	Index	Type of Regression	R^2	RMSE [kg grain N uptake ha^{-1}]	RMSE [%]	MAE [kg grain N uptake ha^{-1}]	Proportion of data points (%) outside of the agronomically relevant interval [$\hat{y}_i \pm 25$ kg grain N uptake ha^{-1}]
2018	51	NDVI	lin	0.00 * **	17.8	15.1	15.2	20.8
2018	51	NDRE	lin	0.03 * **	17.5	14.9	14.3	16.7
2018	51	NIR/GREEN	lin	0.00 * **	17.8	15.1	15.0	16.7
2018	51	NIR/RED	lin	0.00 * **	17.8	15.1	15.2	20.8
2018	51	NIR/REDEDGE	lin	0.04 * **	17.5	14.8	14.2	16.7
2018	61	NDVI	lin	0.04 * **	17.4	14.8	13.7	20.8
2018	61	NDRE	lin	0.20 * **	15.9	13.5	12.4	8.3
2018	61	NIR/GREEN	lin	0.25 * **	15.4	13.1	11.2	8.3
2018	61	NIR/RED	lin	0.05 * **	17.4	14.8	13.7	20.8
2018	61	NIR/REDEDGE	lin	0.20 * **	15.9	13.5	12.3	8.3
2019	36	NDVI	lin	0.22 * **	21.2	14.3	17.2	20.7
2019	36	NDRE	lin	0.45 * **	17.8	12.1	13.9	17.2
2019	36	NIR/GREEN	lin	0.50 * **	16.9	11.4	13.2	10.3
2019	36	NIR/RED	lin	0.25 * **	20.8	14.1	16.8	20.7
2019	36	NIR/REDEDGE	lin	0.44 * **	18.0	12.1	14.0	17.2
2019	86	NDVI	poly	0.73 * **	13.2	9.1	10.5	6.3
2019	86	NDRE	poly	0.75 * **	12.5	8.6	10.4	3.1
2019	86	NIR/GREEN	poly	0.72 * **	13.3	9.1	11.1	9.4
2019	86	NIR/RED	lin	0.71 * **	13.7	9.4	11.0	9.4
2019	86	NIR/REDEDGE	poly	0.75 * **	12.6	8.7	10.5	3.1

NNI (Table 5), and grain yield (Table 6) were evaluated using statistical measures of goodness.

In both years, more linear than polynomial regressions were observed across all traits and measurement dates. The R^2 values ranged from 0.00 (not significant) to 0.75 (highly significant). Independent of the trait, higher R^2 values were observed, particularly in 2019, which were markedly increased at BBCH 86.

Across all measurement dates in both years, the RMSE and MAE values for the above-ground N uptake ranged from 14.7 to 36.9 and from 10.0 to 29.9 kg N ha^{-1}, respectively. All standardized RMSE values were rated as good, and the proportion of data points falling outside the agronomic interval ranged from 4.2% to 31.3% and was markedly higher in 2019. For grain N uptake, the RMSE and MAE values ranged from 12.7 to 21.2 and 11.2–16.8 kg N ha^{-1}. The standardized RMSE values for both measurement dates in 2018 and at BBCH 36 in 2019 were rated as good, and at BBCH 86 in 2019 were rated as excellent. Regarding grain N uptake, the proportion of data points falling outside the agronomic interval ranged from 3.1% to 20.8% and was lower at later growth stages during both years. The RMSE and MAE values for the NNI ranged from 0.07 to 0.18 and from 0.06 to 0.15, and the standardized RMSE values were rated as good, except for the excellent rating at BBCH 86 in 2019. The NNI, which had the lowest proportion of data

Table 5
Comparison of statistical measures of goodness depicting the spectral assessment of the NNI of maize in different years and development stages (* ≙ $p < 0.05$, and *** ≙ $p < 0.001$). $\hat{y}_i$ is the estimator of the polynomial (poly) and linear (lin) regression function at the point x_i.

Year	BBCH	Index	Type of Regression	R^2	RMSE [NNI units]	RMSE [%]	MAE [NNI units]	Proportion of data points (%) outside of the agronomically relevant interval [$\hat{y}_i \pm 0.2$ NNI]
2018	51	NDVI	lin	0.01 * **	0.14	14.2	0.11	16.7
2018	51	NDRE	poly	0.10 * **	0.14	13.5	0.10	12.5
2018	51	NIR/GREEN	poly	0.09 * **	0.14	13.6	0.10	12.5
2018	51	NIR/RED	lin	0.00 * **	0.14	14.2	0.11	16.7
2018	51	NIR/REDEDGE	poly	0.10 * **	0.14	13.5	0.10	12.5
2018	61	NDVI	lin	0.00 * **	0.13	13.1	0.10	12.5
2018	61	NDRE	lin	0.10 * **	0.13	12.5	0.10	12.5
2018	61	NIR/GREEN	lin	0.06 * **	0.13	12.7	0.11	16.7
2018	61	NIR/RED	lin	0.00 * **	0.13	13.1	0.10	12.5
2018	61	NIR/REDEDGE	lin	0.09 * **	0.13	12.5	0.10	12.5
2019	36	NDVI	lin	0.12 * **	0.18	15.9	0.15	31.0
2019	36	NDRE	lin	0.39 * **	0.15	13.2	0.13	17.2
2019	36	NIR/GREEN	lin	0.38 * **	0.15	13.4	0.12	17.2
2019	36	NIR/RED	lin	0.15 * **	0.18	15.7	0.15	31.0
2019	36	NIR/REDEDGE	lin	0.39 * **	0.15	13.3	0.13	17.2
2019	86	NDVI	lin	0.58 * **	0.09	11.1	0.07	3.2
2019	86	NDRE	lin	0.74 * **	0.07	8.8	0.06	0.0
2019	86	NIR/GREEN	lin	0.68 * **	0.08	9.7	0.07	0.0
2019	86	NIR/RED	lin	0.58 * **	0.10	11.2	0.08	3.2
2019	86	NIR/REDEDGE	lin	0.74 * **	0.08	8.8	0.06	0.0

Table 6
Comparison of statistical measures of goodness depicting the spectral assessment of maize yield [t ha^{-1}] in different years and development stages (** ≙ $p < 0.01$, and *** ≙ $p < 0.001$). $\hat{y}_i$ is the estimator of the polynomial (poly) and linear (lin) regression function at the point x_i.

Year	BBCH	Index	Type of Regression	R^2	RMSE [t ha^{-1}]	RMSE [%]	MAE [t ha^{-1}]	Proportion of data points (%) outside of the agronomically relevant interval [$\hat{y}_i \pm 1.4$ t ha^{-1}]
2018	51	NDVI	lin	0.00 * **	1.1	10.4	1.0	16.7
2018	51	NDRE	lin	0.03 * **	1.1	10.2	0.9	16.7
2018	51	NIR/GREEN	lin	0.00 * **	1.1	10.4	1.0	16.7
2018	51	NIR/RED	lin	0.00 * **	1.1	10.4	1.0	16.7
2018	51	NIR/REDEDGE	lin	0.03 * **	1.1	10.2	0.9	16.7
2018	61	NDVI	lin	0.05 * **	1.1	10.1	0.9	16.7
2018	61	NDRE	lin	0.11 * **	1.1	9.8	0.8	16.7
2018	61	NIR/GREEN	lin	0.10 * **	1.1	9.8	0.8	16.7
2018	61	NIR/RED	lin	0.05 * **	1.1	10.1	0.9	12.5
2018	61	NIR/REDEDGE	lin	0.11 * **	1.1	9.8	0.8	16.7
2019	36	NDVI	lin	0.30 * **	1.2	8.8	0.9	17.2
2019	36	NDRE	lin	0.48 * **	1.0	7.6	0.8	17.2
2019	36	NIR/GREEN	lin	0.51 * **	1.0	7.4	0.8	17.2
2019	36	NIR/RED	lin	0.32 * **	1.2	8.7	0.9	17.2
2019	36	NIR/REDEDGE	poly	0.51 * **	1.0	7.4	0.8	24.1
2019	86	NDVI	lin	0.64 * **	0.9	6.7	0.7	9.4
2019	86	NDRE	lin	0.60 * **	1.0	7.1	0.8	9.4
2019	86	NIR/GREEN	lin	0.63 * **	0.9	6.8	0.7	12.5
2019	86	NIR/RED	lin	0.63 * **	0.9	6.8	0.7	9.4
2019	86	NIR/REDEDGE	lin	0.59 * **	1.0	7.2	0.8	9.4

points falling outside the agronomic interval compared to all traits, ranged from 0.0% to 31.0% and was lower at BBCH 86, especially in 2019. Regarding grain yield, the RMSE and MAE values ranged from 0.9 to 1.2 and from 0.7 to 1.0 t ha^{-1}, respectively. The standardized RMSE values in BBCH 51 in 2018 were rated as good, in BBCH 61 in 2018 as good to excellent, and at both measurement dates in 2019 as excellent. The proportion of data points that fell outside the agronomic interval for grain yield ranged from 9.4% to 24.1% and was slightly lower at later growth stages, especially in 2019.

Regardless of the development stage and year, the RMSE values were generally higher than the MAE values. However, within one date*year combination, higher R^2 values were associated with lower RMSE and MAE values and fewer data points outside the agronomic interval.

Generally, the influence of the developmental stage and year was greater than the effect of the specific trait. In addition, the detectability of the traits grain yield and grain N uptake increased at later developmental stages during both years.

4. Discussion

4.1. Weather conditions, soil nitrate-N contents, and plant development

Although the average temperature was slightly above the long-term average during both years, an additional examination of daily average temperatures (data not shown) did not reveal any extreme values, e.g., above 30 °C, which might negatively influence maize growth (Stewart et al., 1998). Moreover, no maize plant stress symptoms were observed during both years. The prevailing temperatures seemed to favorably

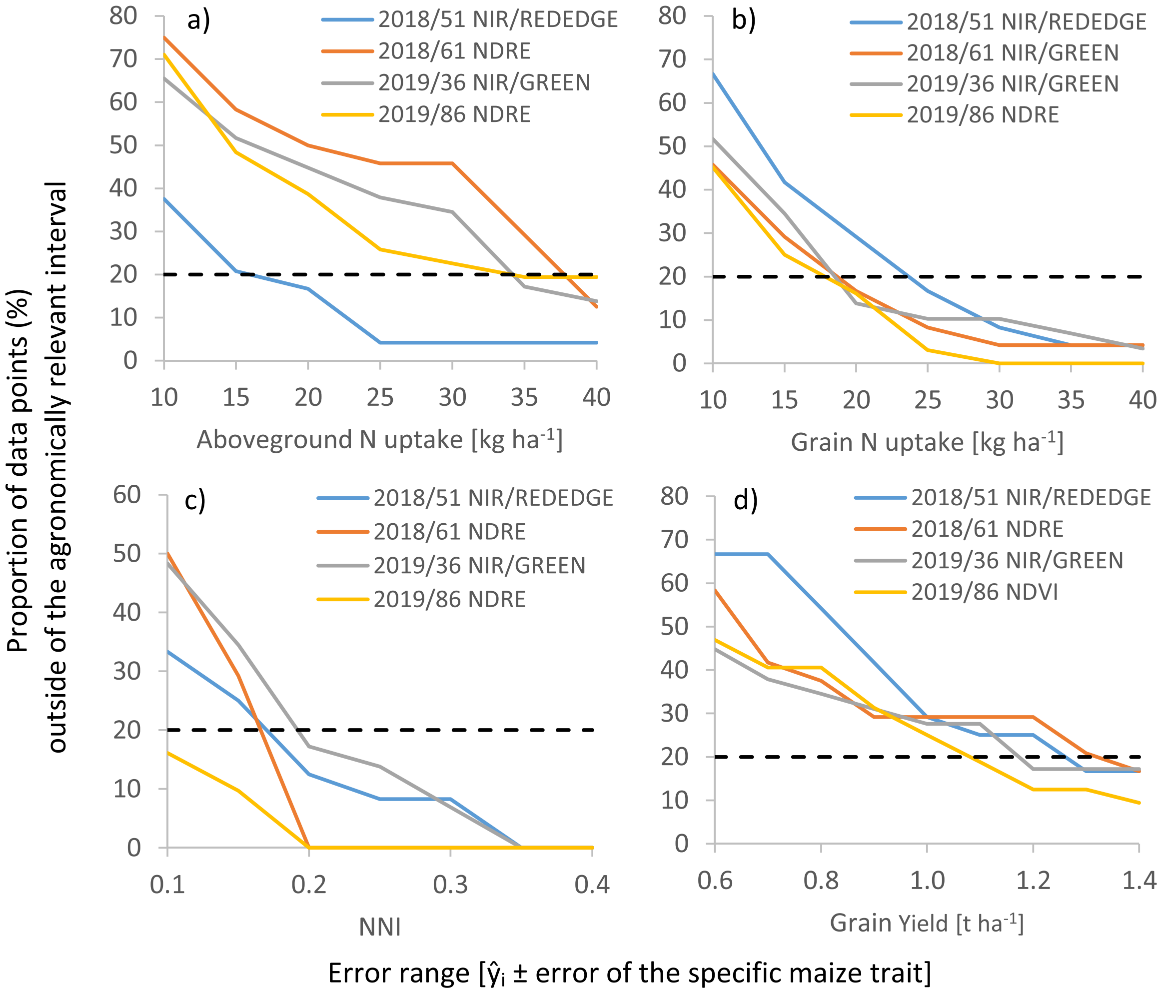

Fig. 5. Sensitivity analysis of agronomically considered appropriate intervals for N-related traits (a) above-ground N uptake [kg N ha^{-1}], (b) grain N uptake [kg N ha^{-1}], (c) NNI, and d) grain yield [t ha^{-1}] of maize. The best-performing index is indicated according to conventional statistics at each date*trait combination. The dashed lines indicate the threshold value of 20% of data points outside the agronomically relevant interval. $\hat{y}_i$ is the estimator of the polynomial (poly) and linear (lin) regression function at the point x_i.

support maize growth, resulting in high yields, given that the site-specific yield expectations ranged from 9–12 t ha^{-1}. In addition, the lower precipitation level was considered to have had little effect on growth during both years. The soil (Cambisol) at this site has a high available field capacity (down to 100 cm soil depth of around 241 mm), which is attained at the beginning of vegetation and buffers a possible lack of precipitation (Heil et al., 2020). Other authors also reported a strong influence of soil factors and year effects for maize growth (Di Paolo and Rinaldi, 2008; Berenguer et al., 2009; Correndo et al., 2021).

The high N supply of the soil in 2018 and 2019 at this site, which cannot be explained by long-term organic fertilization, was astonishing. However, this observation was in line with other studies reporting an indigenous N supply of 80–240 kg N ha^{-1} for maize (Cassman et al., 2002). Nevertheless, an effect of N-fertilization was evident from the increased N uptake in the fertilized variants (Fig. 4). In agreement with Mistele and Schmidhalter (2008), the N uptake can be considered normal for this site in both years. Additionally, the authors observed a surprisingly high soil N supply for maize at the same site during one year, which could be attributed to residual soil N from the previous year, which had been very dry. However, this observation can be excluded from this study. Osterholz et al. (2017) observed that the daily gross ammonification rate of the soil exceeds the daily N uptake of maize. It is further suggested that maize can efficiently utilize this N source in competition with soil microbes and thereby cover its N uptake. In this study, the necessary organic matter would have been present at both sites, although no organic fertilization was carried out. Quan et al. (2021) evaluated field ^{15}N tracer studies for maize in a meta-analysis and emphasized the importance of soil organic C in increasing N use efficiency. However, a high proportion of organic matter in the soil does not necessarily mean sufficient N replenishment. In Europe, more than 40% of the N uptake of maize is derived from N-fertilizers, which again emphasizes the importance of N-fertilization.

The nitrate-N content at the beginning of vegetation was significant to be included in the further N-fertilizer requirement determinations in both years. The post-harvest nitrate-N content varied greatly between years and between N levels only during 2018. These results indicate the great influence of both the year and the N-fertilization effects and are in line with Fang et al. (2006), who observed a higher nitrate-N leaching risk in maize than wheat. The potential for nitrate leaching is present when nitrate accumulates in the soil profile or is followed by high drainage periods. For maize, this can affect the periods of spring, autumn, and winter (Di and Cameron, 2002).

4.2. Sensitivity of indices used to detect N-related traits in maize spectrally

This study used a UAV equipped with a multispectral camera to record spectral images from the maize canopy at different developmental stages. Subsequently, commonly used indices (normalized difference, simple ratio) were calculated based on the spectral data to estimate maize traits via regression analysis.

The findings suggest that indices using the GREEN, REDEDGE, and NIR bands performed best. The band RED was less suitable. All traits were able to be spectrally detected similarly. For grain yield, other studies have observed the best performing indices across a wide range of growth stages as those using band combinations of GREEN, RED, NIR, and MIDINFRARED (Osborne et al., 2002; Maresma et al., 2016). For above-ground and grain N uptake, indices using the REDEDGE and NIR region have been shown to be more suitable (Mistele and Schmidhalter, 2008; Li et al., 2014; Becker et al., 2020; Li et al., 2020). The NNI was best determined with indices using GREEN and REDEDGE bands (Zhao et al., 2018). These results indicate the importance of the GREEN spectral band, especially the REDEDGE and NIR bands, in recording the N-related traits of maize. The insensitivity of indices using reflectance in the red region due to low variation in chlorophyll absorption in a dense canopy was in line with previous reports (Gitelson, 2004; Hatfield et al., 2008; Nguy-Robertson et al., 2012).

It is well known that soil (Huete, 1988) and shadow (Zhang et al., 2015) influence spectral indices. Especially concerning the spectral imagery of maize and particularly during early growth stages, other authors have reported the benefits of classifying pixels into the categories of plant, soil, and shadow (Thompson and Puntel, 2020). This study evaluated supervised and unsupervised classification tools of the ArcGIS program (ESRI®, Germany, Version 10.5.0.6491) but with mixed results because many pixels were assigned to incorrect classes (data not shown). Additionally, the SAVI (Huete, 1988) and OSAVI index (Li et al., 2010) were calculated for all dates, but they showed no improvement in sensitivity (data not shown). We assume that, especially during the early growth stages, the error due to soil and shadowing is negligible because very low differences in above-ground biomass were observed across N levels (data not shown). Spectral measurements during midday should reduce possible shadow effects.

4.3. Assessment of regression models evaluating the relationships between spectral measurements and N-related traits (above-ground and grain N uptake, and NNI) as well as grain yield and the adoption of additional agronomic aspects

Regression analysis is commonly used to model the spectral detectability of maize traits, and the models are then often evaluated based on the R^2 values (Mistele and Schmidhalter, 2008; Winterhalter et al., 2011; Maresma et al., 2016; Corti et al., 2019). Furthermore, this study used self-defined agronomic intervals to evaluate the models in addition to well-known statistics such as RMSE and MAE values.

The expression of the R^2 depends mostly on the treatment effect (e.g., N-fertilization). Especially for N, the treatment effect depends on the year (weather), location (e.g., soil), and mainly on the crop's growth stage at the respective measurement date. Across two years and sites and for four different developmental stages of maize, this study observed only slight treatment effects through different N applications, which increased during the course of vegetation. The differentiation of the respective trait through the treatment effect influences the R^2. This is probably because the proportion of the explained deviation sum of squares increases more than the total deviation sum of squares to be explained. Corti et al. (2019) also observed higher R^2 values in later growth stages. However, high R^2 values alone do not generally imply that the trait can be captured well from an agronomical point of view. One additional measure of model performance is the use of RMSE and MAE values, with the advantage being that the given model error has the same unit as the target trait. The MAE averages the absolute deviations, whereas the RMSE averages the squared deviations. By squaring the errors, measured values further away from the regression equation are weighted more heavily, resulting in the RMSE values being larger than the MAE values. This is also evident in the study by Kayad et al. (2019). However, both of them average the model error, leading to under- and overestimating the measured values. In general, high R^2 values tended to lower RMSE and standardized RMSE values (Nguy-Robertson et al., 2012; Xia et al., 2016; Lee et al., 2020; Li et al., 2020; Skakun et al., 2021). Therefore, we attempted in this study to define error limits from an agronomical perspective. Agronomical intervals have the advantage of the model error being self-defined because the interval limits may vary depending on the trait, site conditions (e.g., yield or N-fertilization levels), year, and also from the interest of application (ex-ante and/or ex-post analysis). For example, Thomason et al. (2007) defined the range between the five to nine and Morris et al. (2018) the six to twelve leaf developmental stage for maize as a window for in-season management decisions (ex-ante) for N-fertilization. In addition to the ex-ante approach, ex-post evaluations (e.g., grain yield differentiation through different N-fertilization levels) can also provide useful information. The range of the agronomic interval can therefore be adjusted according to these approaches, and the evaluation of the model performance can be evaluated based on the level of probability that the measured values are within or outside the interval. In both cases, the agronomic interval supports the evaluation of the applicability of the spectral detection of maize traits.

We assume that the defined agronomical error limits for the N-related traits and grain yield of maize were representative of similar high-yielding sites. For low-yielding conditions, the error limits of the grain yield, in particular, could be smaller because they depend in part on the total expression of the trait itself. This aspect needs further evaluation because it cannot be extrapolated from these data. Furthermore, the error limits are valid for indices using the GREEN, REDEDGE, and NIR bands. Indices combining other bands provided slightly worse results. Additionally, the error limits were relatively stable concerning year and growth stages. This was advantageous, because the regression equations produced in different experiments are location-specific (Corti et al., 2018). Although the year effects on maize growth are well-known, and the development of biomass is of great importance in the spectral sensing of maize traits (Mistele and Schmidhalter, 2008), we observed only small differences in above-ground biomass across the N levels within one measurement date (data not shown). Differences in maize biomass are further affected by seeding density (Mistele and Schmidhalter, 2008). Therefore, we assume that small variations in biomass support the stability of the agronomic error limits.

5. Conclusion

The spectral detection of N-related traits of maize plants can provide useful information for making N-fertilizer management decisions and helping prevent N losses. This study suggests that commonly used statistics such as R^2, RMSE, and MAE are not fully adequate for judging the quality of spectral detection for above-ground and grain N uptake, NNI, and grain yield of maize. This is because the R^2 values are influenced by the trait's differentiation, which is affected by year effects, the growth stage, and the variation in N-fertilization. RMSE and MAE values only average the error and lead, therefore mostly to an under- and overestimation of the measured values. Thus, the extension of these statistics with agronomical evaluations should be considered. Intrinsic confidence intervals, defined as error limits based on agronomical considerations, improve regression models' validity and applicability for ex-ante management decisions and/or ex-post management analysis. Therefore, we defined agronomic error limits for above-ground and grain N uptake, NNI, and grain yield of $\pm$ 40 and $\pm$ 25 kg N ha^{-1}, $\pm$ 0.2, and $\pm$ 1.4 t ha^{-1}, respectively. These error limits were valid across years, growth stages, and spectral indices combining the GREEN, REDEDGE, and NIR bands. The agronomically-based detection limits support the evaluation of N-related traits and grain yield of maize.

Declaration of Competing Interest

The authors declare that they have no known competing financial interests or personal relationships that could have appeared to influence

the work reported in this paper.

Data availability

Data will be made available on request.

Acknowledgements

This work was supported as part of the GreenWindows4_0 project by funds of the Federal Ministry of Food and Agriculture 516 (BMEL) based on a decision of the Parliament of the Federal Republic of Germany via the 517 Federal Office for Agriculture and Food (BLE) under the innovation support program.

References

Aasen, H., Bolten, A., 2018. Multi-temporal high-resolution imaging spectroscopy with hyperspectral 2D imagers—from theory to application. In: Remote Sens. Environ, 205, pp. 374–389. https://doi.org/10.1016/j.rse.2017.10.043.

Ali, M.M., Al-Ani, A., Eamus, D., Tan, D.K.Y., 2017. Leaf nitrogen determination using non-destructive techniques - a review. J. Plant Nutr. 40 (7), 928–953. https://doi.org/10.1080/01904167.2016.1143954.

Awika, J.M., 2011. Major cereal grains production and use around the world. In: Awika, J.M., Piironen, V., Bean, S. (Eds.), Advances in Cereal Science: Implications to Food Processing and Health Promotion, 1089. American Chemical Society, pp. 1–13, 10.1021/bk-2011-1089.ch001.

Barbieri, P.A., Echeverría, H.E., Saínz Rozas, H.R., Andrade, F.H., 2008. Nitrogen use efficiency in maize as affected by nitrogen availability and row spacing. Agron. J. 100 (4), 1094–1100. https://doi.org/10.2134/agronj2006.0057.

Barnes, E.M., et al., 2000. Coincident Detection of Crop Water Stress, Nitrogen Status and Canopy Density Using Ground-based Multispectral Data. In: Robert, P.C., Rust, R.H., Larson, W.E. (Eds.), Proc. of the Fifth Int. Conf. on Precis. Agric. Bloomington, MN, USA, pp. 1–15.

Bayerische Landesanstalt für Landwirtschaft (LfL) (2018). Leitfaden für die Düngung von Acker- und Grünlandflächen (Gelbes Heft).

Becker, T., Nelsen, T.S., Leinfelder-Miles, M., Lundy, M.E., 2020. Differentiating between nitrogen and water deficiency in irrigated maize using a UAV-based multispectral camera. Agronomy 10 (11), 1671. https://doi.org/10.3390/agronomy10111671.

Berenguer, P., Santiveri, F., Boixadera, J., Lloveras, J., 2009. Nitrogen fertilization of irrigated maize under Mediterranean conditions. Eur. J. Agron. 30 (3), 163–171. https://doi.org/10.1016/j.eja.2008.09.005.

Bleymüller J., Gehlert G., Gülicher H. (2008). Statistik für Wirtschaftswissenschaftler. Franz Vahlen. 15. Auflage.

Cassman, K.G., Dobermann, A., Walters, D.T., 2002. Agroecosystems, nitrogen-use efficiency, and nitrogen management. J. Hum. Environ. 31 (2), 132–140. https://doi.org/10.1579/0044-7447-31.2.132.

Chen, Y., Xiao, C., Wu, D., Xia, T., Chen, Q., Chen, F., Yuan, L., Mi, G., 2015. Effects of nitrogen application rate on grain yield and grain nitrogen concentration in two maize hybrids with contrasting nitrogen remobilization efficiency. Eur. J. Agron. 62, 79–89. https://doi.org/10.1016/j.eja.2014.09.008.

Ciampitti, I.A., Vyn, T.J., 2011. A comprehensive study of plant density consequences on nitrogen uptake dynamics of maize plants from vegetative to reproductive stages. Field Crops Res. 121 (1), 2–18. https://doi.org/10.1016/j.fcr.2010.10.009.

Climate Data Center (CDC) (2020). Retrieved from 〈https://www.dwd.de/DE/klimaumwelt/cdc/cdc_node.html〉.

Correndo, A.A., Rotundo, J.L., Tremblay, N., Archontoulis, S., Coulter, J.A., Ruiz-Diaz, D., Franzen, D., Franzluebbers, A.J., Nafziger, E., Schwalbert, R., Steinke, K., Williams, J., Messina, C.D., Ciampitti, I.A., 2021. Assessing the uncertainty of maize yield without nitrogen fertilization. Field Crops Res. 260, 107985 https://doi.org/10.1016/j.fcr.2020.107985.

Corti, M., Cavalli, D., Cabassi, G., Gallina, P.M., Bechini, L., 2018. Does remote and proximal optical sensing successfully estimate maize variables? a review. Eur. J. Agron. 99, 37–50. https://doi.org/10.1016/j.eja.2018.06.008.

Corti, M., Cavalli, D., Cabassi, G., Vigoni, A., Degano, L., Gallina, P.M., 2019. Application of a low-cost camera on a UAV to estimate maize nitrogen-related variables. Prec. Agric. 20 (4), 675–696. https://doi.org/10.1007/s11119-018-9609-y. Bundesministerium für Umwelt, N. B., & Landwirtschaft, B. f. (2017, 01). Nitratbericht 2016.

De Souza, R., Buchhart, C., Heil, K., Plass, J., Padilla, F.M., Schmidhalter, U., 2021. Effect of time of day and sky conditions on different vegetation indices calculated from active and passive sensors and images taken from UAV. Remote Sens. 13, 1691. https://doi.org/10.3390/rs13091691.

Di, H.J., Cameron, K.C., 2002. Nitrate leaching in temperate agroecosystems: sources, factors and mitigating strategies. Nutr. Cycl. Agroecosyst 64 (3), 237–256. https://doi.org/10.1023/A:1021471531188.

Di Paolo, E., Rinaldi, M., 2008. Yield response of corn to irrigation and nitrogen fertilization in a Mediterranean environment. Field Crops Res. 105 (3), 202–210. https://doi.org/10.1016/j.fcr.2007.10.004.

Dordas, C.A., Lithourgidis, A.S., Matsi, T., Barbayiannis, N., 2008. Application of liquid cattle manure and inorganic fertilizers affect dry matter, nitrogen accumulation, and partitioning in maize. Nutr. Cycl. Agroecosyst. 80 (3), 283–296. https://doi.org/10.1007/s10705-007-9143-1.

Erenstein, O., Chamberlin, J., Sonder, K., 2021. Estimating the global number and distribution of maize and wheat farms. Glob. Food Sec. 30, 100558 https://doi.org/10.1016/j.gfs.2021.100558.

Fageria, N.K., Baligar, V.C., 2005. Enhancing nitrogen use efficiency in crop plants. Adv. in Agron 88, 97–185. https://doi.org/10.1016/S0065-2113(05)88004-6.

Fang, Q., Yu, Q., Wang, E., Chen, Y., Zhang, G., Wang, J., Li, L., 2006. Soil nitrate accumulation, leaching and crop nitrogen use as influenced by fertilization and irrigation in an intensive wheat–maize double cropping system in the North China Plain. Plant Soil 284 (1), 335–350. https://doi.org/10.1007/s11104-006-0055-7.

Galloway, J.N., Townsend, A.R., Erisman, J.W., Bekunda, M., Cai, Z., Freney, J.R., Matinelli, L.A., Seitzinger, S.P., Sutton, M.A., 2008. Transformation of the Nitrogen Cycle: Recent Trends, Questions, and Potential Solutions. Science 320, 889–892. https://doi.org/10.1126/science.1136674.

García-Martínez, H., Flores-Magdaleno, H., Ascencio-Hernández, R., Khalil-Gardezi, A., Tijerina-Chávez, L., Mancilla-Villa, O.R., Vázquez-Peña, M.A., 2020. Corn grain yield estimation from vegetation indices, canopy cover, plant density, and a neural network using multispectral and RGB images acquired with unmanned aerial vehicles. doi.org/ Agric. 10 (7), 277. https://doi.org/10.3390/agriculture10070277.

Gitelson, A.A., 2004. Wide dynamic range vegetation index for remote quantification of biophysical characteristics of vegetation. J. Plant Physiol. 161 (2), 165–173. https://doi.org/10.1078/0176-1617-01176.

Gitelson, A.A., Viña, A., Arkebauer, T.J., Rundquist, D.C., Keydan, G., Leavitt, B., 2003. Remote estimation of leaf area index and green leaf biomass in maize canopies. Geophys. Res. Lett. 30 (5), 1248. https://doi.org/10.1029/2002GL016450.

Gnädinger, F., Schmidhalter, U., 2017. Digital counts of maize plants by unmanned aerial vehicles (UAVs). Remote Sens. 9 (6), 544. https://doi.org/10.3390/rs9060544.

Hatfield, J.L., Gitelson, A.A., Schepers, J.S., Walthall, C.L., 2008. Application of spectral remote sensing for agronomic decisions. Agron. J. 100, 117–131. https://doi.org/10.2134/agronj2006.0370c.

Heil, K., Lehner, A., Schmidhalter, U., 2020. Influence of Climate Conditions on the Temporal Development of Wheat Yields in a Long-Term Experiment in an Area with Pleistocene Loess. Climate 8 (9), 100. https://doi.org/10.3390/cli8090100.

Heinemann, P., Schmidhalter, U., 2021. Simplifying residual nitrogen (N_{min}) sampling strategies and crop response. Eur. J. Agron. 130, 126369 https://doi.org/10.1016/j.eja.2021.126369.

Hu, Y., Knapp, S., Schmidhalter, U., 2020. Advancing high-throughput phenotyping of wheat in early selection cycles. Remote Sens 12, 574. https://doi.org/10.3390/rs12030574.

Huete, A.R., 1988. A soil-adjusted vegetation index (SAVI. Remote Sens. Environ. 25, 295–309. https://doi.org/10.1016/0034-4257(88)90106-X.

Hunt Jr., E.R., Daughtry, C.S., 2018. What good are unmanned aircraft systems for agricultural remote sensing and precision agriculture? Int. J. Remote Sens. 39 (15-16), 5345–5376. https://doi.org/10.1080/01431161.2017.1410300.

Kayad, A., Sozzi, M., Gatto, S., Marinello, F., Pirotti, F., 2019. Monitoring within-field variability of corn yield using Sentinel-2 and machine learning techniques. Remote Sens. 11 (23), 2873. https://doi.org/10.3390/rs11232873.

Köhler W., Schachtel G., Voleske P. (2012). Biostatistik: Eine Einführung für Biologen und Agrarwissenschaftler. Springer Spektrum, 5. Auflage.

Ladha, J.K., Pathak, H., Krupnik, T.J., Six, J., van Kessel, C., 2005. Efficiency of Fertilizer Nitrogen in Cereal Production: Retrospects and Prospects. Adv. in Agron Vol. 87, 85–156. https://doi.org/10.1016/S0065-2113(05)87003-8.

Lee, H., Wang, J., Leblon, B., 2020. Using linear regression, Random Forests, and Support Vector Machine with unmanned aerial vehicle multispectral images to predict canopy nitrogen weight in corn. Remote Sens. 12 (13), 2071. https://doi.org/10.3390/rs12132071.

Lemaire, G., Gastal, F., 1997. N uptake and distribution in plant canopies. In: Lemaire, G. (Ed.), Diagnosis of the nitrogen status in crops. Springer-Verlag, Berlin, Heidelberg, pp. 3–43. https://doi.org/10.1007/978-3-642-60684-7.

Li, F., Elsayed, S., Hu, Y., Schmidhalter, U., 2020. Passive reflectance sensing using optimized two-and three-band spectral indices for quantifying the total nitrogen yield of maize. Comput. Electron. Agric. 173, 105403 https://doi.org/10.1016/j.compag.2020.105403.

Li, F., Miao, Y., Henning, S.D., Gnyp, M.L., Chen, X., Jia, L., Bareth, G., 2010. Evaluating hyperspectral vegetation indices for estimating nitrogen concentration of winter wheat at different growth stages. Prec. Agri. 11, 335–357. https://doi.org/10.1007/s11119-010-9165-6.

Li, F., Miao, Y., Feng, G., Yuan, F., Yue, S., Gao, X., Liu, Y., Liu, B., Ustin, S.L., Chen, X., 2014. Improving estimation of summer maize nitrogen status with red edge-based spectral vegetation indices. Field Crops Res. 157, 111–123. https://doi.org/10.1016/j.fcr.2013.12.018.

Lilienthal, H., 2014. Optical sensors in agriculture: Principles and concepts. J. für Kulturpflanzen 66 (2), 34–41. https://doi.org/10.5073/JFK.2014.02.01.

Loague, K., Green, R.E., 1991. Statistical and graphical methods for evaluating solute transport models: Overview and application. J. Contam. Hydrol. 7 (1-2), 51–73. https://doi.org/10.1016/0169-7722(91)90038-3.

Maresma, Á., Ariza, M., Martínez, E., Lloveras, J., Martínez-Casasnovas, J.A., 2016. Analysis of vegetation indices to determine nitrogen application and yield prediction in maize (Zea mays L.) from a standard UAV service. Remote Sens. 8 (12), 973. https://doi.org/10.3390/rs8120973.

Mason, S.C., D`croz-Mason, N.E., 2002. Agronomic practices influence maize grain quality. J. Crop Prod. 5 (1-2), 75–91. https://doi.org/10.1300/J144v05n01_04.

Meier, U., 2018. Growth stages of mono- and dicotyledonous plants: BBCH Monograph. Julius Kühn-Institut (JKI).

Mistele, B., Schmidhalter, U., 2008. Spectral measurements of the total aerial N and biomass dry weight in maize using a quadrilateral-view optic. Field Crops Res. 106 (1), 94–103. https://doi.org/10.1016/j.fcr.2007.11.002.
Morris, T.F., et al., 2018. Strengths and limitations of nitrogen rate recommendations for corn and opportunities for improvement. Agron. J. 110 (1), 1. https://doi.org/10.2134/agronj2017.02.0112.
Nguy-Robertson, A., Gitelson, A., Peng, Y., Viña, A., Arkebauer, T., Rundquist, D., 2012. Green leaf area index estimation in maize and soybean: Combining vegetation indices to achieve maximal sensitivity. Agron. J. 104 (5), 1336–1347. https://doi.org/10.2134/agronj2012.0065.
Osborne, S.L., Schepers, J.S., Francis, D.D., Schlemmer, M.R., 2002. Use of spectral radiance to estimate in-season biomass and grain yield in nitrogen- and water-stressed corn. Crop Sci. 42 (1), 165–171. https://doi.org/10.2135/cropsci2002.1650.
Osterholz, W.R., Rinot, O., Liebman, M., Castellano, M.J., 2017. Can mineralization of soil organic nitrogen meet maize nitrogen demand? Plant Soil 415 (1), 73–84. https://doi.org/10.1007/s11104-016-3137-1.
Plénet, D., Lemaire, G., 1999. Relationships between dynamics of nitrogen uptake and dry matter accumulation in maize crops. Determination of critical N concentration. Plant Soil 216 (1), 65–82. https://doi.org/10.1023/A:1004783431055.
Quan, Z., Zhang, X., Davidson, E.A., Zhu, F., Li, S., Zhao, X., Chen, X., Zhang, L.-M., He, J.-Z., Wei, W., Fang, Y., 2021. Fates and use efficiency of nitrogen fertilizer in maize cropping systems and their responses to technologies and management practices: A global analysis on field ^{15}N tracer studies. e2020EF001514. doi.org/Earth's Future 9 (5). https://doi.org/10.1029/2020EF001514.
Ramos, A.P.M., Osco, L.P., Furuya, D.E.G., Gonçalves, W.N., Santana, D.C., Teodoro, L.P.R., da Silva Junior, C.A., Capristo-Silva, G.F., Li, J., Baio, F.H.R., Marcato Junior, J., Teodoro, P.E., Pistori, H., 2020. A random forest ranking approach to predict yield in maize with UAV-based vegetation spectral indices. Comput. Electron. Agric. 178, 105791 https://doi.org/10.1016/j.compag.2020.105791.
Ranum, P., Peña-Rosas, J.P., Garcia-Casal, M.N., 2014. Global maize production, utilization, and consumption. Ann. N. Y. Acad. Sci. 1312 (1), 105–112. https://doi.org/10.1111/nyas.12396.
Raun, W.R., Johnson, G.V., 1999. Improving nitrogen use efficiency for cereal production. Agron. J. 91 (3), 357–363. https://doi.org/10.2134/agronj1999.00021962009100030001x.
Robertson, G.P., Vitousek, P.M., 2009. Nitrogen in agriculture: balancing the cost of an essential resource ressource. Annu. Rev. Environ. Resour. (34), 97–125. https://doi.org/10.1146/annurev.environ.032108.105046.
Rouse J.W., Haas R.H., Schell J.A., Deering D.W., Harlan J.C. (1974). Monitoring the vernal Advancement of Retrogradation of natural vegetation. Report No. E75-10354. Washington, DC: NASA.
Schmidhalter U., Glas J., Heigl R., Manhart R., Wiesent S., Gutser R., Neudecker E. (2001). Application and testing of a crop scanning instrument - field experiments with reduced crop width, tall maize plants and monitoring of cereal yield. In: Grenier G., Blackmore S. (Eds.) Third european conference on precision agriculture, June 18-20, 2001, Montpellier, France, p. 953-958.
Skakun, S., Kalecinski, N.I., Brown, M.G., Johnson, D.M., Vermote, E.F., Roger, J.C., Franch, B., 2021. Assessing within-Field Corn and Soybean Yield Variability from WorldView-3, Planet, Sentinel-2, and Landsat 8 Satellite Imagery. Remote Sens. 13 (5), 872. https://doi.org/10.3390/rs13050872.
Stewart, D.W., Dwyer, L.M., Carrigan, L.L., 1998. Phenological temperature response of maize. Agron. J. 90 (1), 73–79. https://doi.org/10.2134/agronj1998.00021962009000010014x.
Teal, R.K., Tubana, B., Girma, K., Freeman, K.W., Arnall, D.B., Walsh, O., Raun, W.R., 2006. In-season prediction of corn grain yield potential using normalized difference vegetation index. Agron. J. 98 (6), 1488–1494. https://doi.org/10.2134/agronj2006.0103.
Thomason, W.E., Phillips, S.B., Raymond, F.D., 2007. Defining useful limits for spectral reflectance measures in corn. J. Plant Nutr. 30 (8), 1263–1277. https://doi.org/10.1080/01904160701555176.
Thompson, L.J., Puntel, L.A., 2020. Transforming Unmanned Aerial Vehicle (UAV) and Multispectral Sensor into a Practical Decision Support System for Precision Nitrogen Management in Corn. Remote Sens. 12 (10), 1597. https://doi.org/10.3390/rs12101597.
Thompson, L.J., Ferguson, R.B., Kitchen, N., Frazen, D.W., Mamo, M., Yang, H., Schepers, J.S., 2015. Model and sensor-based recommendation approaches for in-season nitrogen management in corn. Agron. J. 107, 2020–2030. https://doi.org/10.2134/agronj15.0116.
Walburg, G.M.M.E., Bauer, M.E., Daughtry, C.S.T., Housley, T.L., 1982. Effects of nitrogen nutrition on the growth, yield, and reflectance characteristics of corn canopies. Agron. J. 74 (4), 677–683. https://doi.org/10.2134/agronj1982.00021962007400040020x.
Webster, R., McBratney, A.B., 1989. On the Akaike information criterion for choosing models for variograms of soil properties. J. Soil Sci 40, 493–496. https://doi.org/10.1111/j.1365-2389.1989.tb01291.x.
Westermeier, M., Maidl, F.-X., 2019. Comparison of spectral indices to detect nitrogen uptake in winter wheat. J. für Kulturpflanzen 71 (8-9), 238–248. https://doi.org/10.5073/JfK.2019.08-09.02.
Willmott, C.J., 1984. On the evaluation of model performance in physical geography. Spatial statistics and models. Springer, Dordrecht, pp. 443–460. https://doi.org/10.1007/978-94-017-3048-8_23.
Winterhalter, L., Mistele, B., Schmidhalter, U., 2013. Evaluation of active and passive sensor systems in the field to phenotype maize hybrids with high-throughput. Field Crops Res. 154, 236–245. https://doi.org/10.1016/j.fcr.2013.09.006.
Winterhalter, L., Mistele, B., Jampatong, S., Schmidhalter, U., 2011. High-throughput sensing of aerial biomass and above-ground nitrogen uptake in the vegetative stage of well-watered and drought-stressed tropical maize hybrids. Crop Sci. 51, 479–489. https://doi.org/10.2135/cropsci2010.07.0397.
Xia, T., Miao, Y., Wu, D., Shao, H., Khosla, R., Mi, G., 2016. Active optical sensing of spring maize for in-season diagnosis of nitrogen status based on nitrogen nutrition index. Rem. Sens. 8 (7), 605. https://doi.org/10.3390/rs8070605.
Zaman-Allah, M., Vergara, O., Araus, J.L., Tarekegne, A., Magorokosho, C., Zarco-Tejada, P.J., Hornero, A., Hernández Albá, A., Das, B., Craufurd, P., Olsen, M., Prasanna, B.M., Cairns, J., 2015. Unmanned aerial platform-based multispectral imaging for field phenotyping of maize. Plant Methods 11 (1), 1–10. https://doi.org/10.1186/s13007-015-0078-2.
Zhang, L., Sun, X., Wu, T., Zhang, H., 2015. An analysis of shadow effects on spectral vegetation indexes using a ground-based imaging spectrometer. IEEE Geosci. Remote Sens. Letters 12 (11), 2188–2192. https://doi.org/10.1109/LGRS.2015.2450218.
Zhang, M., Zhou, J., Sudduth, K.A., Kitchen, N.R., 2020. Estimation of maize yield and effects of variable-rate nitrogen application using UAV-based RGB imagery. Bios. Eng. 189, 24–35. https://doi.org/10.1016/j.biosystemseng.2019.11.001.
Zhao, B., Duan, A., Ata-Ul-Karim, S.T., Liu, Z., Chen, Z., Gong, Z., Zhang, J., Xiao, J., Liu, Z., Qin, A., Ning, D., 2018. Exploring new spectral bands and vegetation indices for estimating nitrogen nutrition index of summer maize. Eur. J. Agron. 93, 113–125. https://doi.org/10.1016/j.eja.2017.12.006.